JPNT 5(4), 173-180 (2016)
https://doi.org/10.11003/JPNT.2016.5.4.173

JPNT Journal of Positioning, Navigation, and Timing

Multipath Mitigation for Pulses Using Supervised Learning: Application to Distance Measuring Equipment

Euiho Kim†

Department of Aeronautical and Mechanical Engineering, Cheongju University, Cheongju 28503, Korea

ABSTRACT

This paper presents a method to suppress multipath induced by pulses using supervised learning. In modern electronics, pulses have been used for various purposes such as communication or distance measurements. Like other signals, pulses also suffer from multipath. When a pulse and a multipath are overlapped, the original pulse shape is distorted. The distorted pulse could result in communication failures or distance measurement errors. However, a large number of samples available from a pulse can be used to effectively reject multipath by using a supervised learning method. This paper introduces how a supervised learning method can be applied to Distance Measuring Equipment. Simulation results show that multipath induced distance measuring error can be suppressed by 10 ~ 45 percent depending on the allowed pulse shape variation allowed in a standard.

Keywords: distance measuring equipment, APNT, GNSS, supervised learning

1. INTRODUCTION

Distance Measuring Equipment (DME/Normal or DME/N) is a pulse based ranging system. It consists of airborne and ground subsystems (Kayton & Fried 1997). The airborne subsystem is called an interrogator and the ground subsystem is a transponder. It determines a slant range between the interrogator and the transponder by measuring the two-way flight time in exchanging DME/N pulses. The time of flight or the time of arrival (TOA) is measured with respect to the half amplitude point of the pulse. When a transmitted pulse is distorted, trait is likely that the half amplitude point of the transmitted pulse is shifted, therefore ranging errors may occur. The primary cause of a DME/N pulse distortion is multipath and the multipath induced range errors in DME can be over one hundred meters.

However, rigorous efforts have not been made to suppress DME/N multipath induced range errors. One probable reason is that the required DME/N range accuracy for DME-based en-route and non-precision approach is satisfied without multipath rejection. Recently, Federal Aviation Administration (FAA) in United States has considered DME/N as one of the possible Alternative Position Navigation and Timing (APNT) systems for Global Navigation Satellite Systems (Lo et al. 2011, Kim 2012). The advantage of DME/N as an APNT system is the wide spread DME/N ground station network in U.S. Conterminous. Also, the DME avionics are currently installed in most large aircraft. However, its drawback is that the DME range accuracy is too poor to meet the required APNT position accuracy. To enable DME to have a better range accuracy, there have recently been two major improvements. Pelgrum et al. (2012) has developed a modified DME/N system that utilizes DME carrier as a ranging source. This system could replace the current DME design and be a long term DME solution for APNT. On the other hand, Kim (2013a) proposes alternative DME/N pulses that improves the ranging accuracy against noise and multipath.

Concerning the large DME ranging errors due to multipath, Lo et al. (2014) proposed possible DME/N multipath mitigation methods, which are the modification

Received Oct 11, 2016 **Revised** Nov 10, 2016 **Accepted** Nov 11, 2016
†**Corresponding Author**
E-mail: euihokim@cju.ac.kr
Tel: +82-43-229-8393 Fax: +82-43-229-7955

Copyright © The Korean GNSS Society
http://www.gnss.or.kr Print ISSN: 2288-8187 Online ISSN: 2289-0866

of flight operations and procedures to avoid severe multipath from nearby environment, simple averaging of DME/N range measurements, and carrier smoothing & extended averaging. First, the change of flight operation or procedures seems to be expensive because it requires analysis of DME/N signal propagation in extremely large area. The simple averaging works fine in some cases, but (Lo et al. 2014) found that it worked poorly in a certain DME/N ground station to aircraft geometry. The carrier smoothing & extended averaging may be able to effectively suppress multipath if clock oscillators in DME/N perform very stable. However, most DME/Ns in operation were found to not have clock oscillators stable enough for the carrier smoothing.

As a further effort for DME multipath mitigation, this paper proposes a supervised learning based multipath rejection method (Kim 2013b). The supervised learning is one of the popular machine learning algorithms, whose goal is to find a mapping function for given training data consisting of inputs and outputs (Chapelle et al. 2006). The supervised learning has been widely used in various applications including health science (Ghosh-Dastidar & Adeli 2009, Adeli & Ghosh-Dastidar 2010), speech recognition (Smaragdis 2007), network traffic classification (Erman et al. 2007), and image processing (Carneiro et al. 2007) to name a few.

In this paper, the supervised learning is used to develop an estimator that predicts multipath induced TOA errors from the shape of a received DME pulse. The paper first discusses DME pulse shape and its multipath impact. Then, the DME multipath modeling and the training data generation for learning will be introduced. Next, estimators developed from using the training data and their multipath rejection performance will be discussed.

2. DME PULSE WAVEFORMS AND SUPERVISED LEARNING APPROACH

2.1 DME Pulse Waveform and Multipath Impacts

This section overviews the pulse shape characteristics of DME and its multipath impacts. The DME pulse shape requirements are listed in Table 1 (Kim 2013a) and a standard Gaussian DME pulse is shown in Fig. 1. The standard or reference Gaussian DME pulse has a rise time of 2.5 μs, a width of 3.0 μs, and a fall time of 2.5 μs. In Fig. 1, the reference Gaussian pulse is denoted as a direct pulse and the distorted pulse shape due to multipath is also depicted. The TOA of a DME is determined with respect to the half amplitude point of the pulse. When the pulse shape is distorted due to multipath, the half amplitude point is shifted, therefore the TOA measurement error may be induced.

Table 1. Current DME/N ground transponder pulse shape requirements.

Pulse shape parameters	Range
Rise time	2.5 (+0.5, -1.0) μs
Pulse top	No instantaneous fall below a value which is 95% of the maximum voltage amplitude of the pulse
Pulse duration	3.5 (±0.5) μs
Fall time	2.5 (±0.5) μs

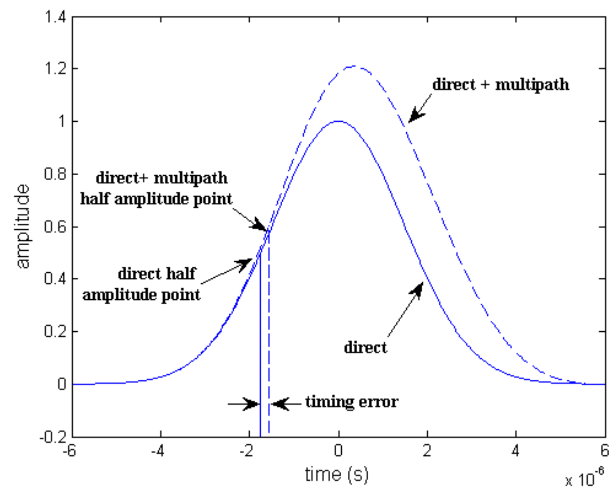

Fig. 1. Gaussian DME/N pulse shape (Kim 2013b).

As an example, the shape of the standard Gaussian pulse in Fig. 1 is distorted due to multipath such that it has a rise time of 2.66 μs, a width of 3.97 μs, and a fall time of 2.86 μs. The half amplitude point of the distorted pulse is 0.19 μs behind the true half amplitude point of the direct pulse. As a result, a range error of 56 m is induced.

However, the distorted pulse shape in Fig. 1 is still valid with respect to the requirements in Table 1. In fact, this type of pulse shape can be transmitted from any DME equipment including airborne interrogators and ground transponders. In that case, an undesirable consequence is that it is hard to determine whether a received pulse keeps the transmitted pulse shape or it is significantly distorted due to multipath. As a result, no further signal processing technique can be performed unless the allowed pulse waveform variation in the specifications is tightened. The issue will be further discussed later in this paper.

2.2 Regression as a Supervised Learning for DME Multipath Suppression

Supervised learning is one of the machine learning techniques that infer a mapping function between a set of input variables and output variables (Carneiro et al. 2007, Cord et al. 2009). Regression is one type of the supervised learning particularly when the output variable is continuous. When a discrete output is used, this type of supervised learning is called a classification. For the multipath suppression problem, a more adequate selection of the supervised learning methods is regression.

The goal of a regression or supervised learning is to infer a function h:$\boldsymbol{X}\rightarrow\boldsymbol{Y}$ from training set D_{n} composed of pairs of (input, output):

$$D_n = ((\boldsymbol{x}_1, y_1), ..., (\boldsymbol{x}_n, y_n)) \in (\boldsymbol{X} \times \boldsymbol{Y})^n \tag{1}$$

$\boldsymbol{x}_i$ belongs to some input set $\boldsymbol{X}\subset\boldsymbol{R}^k$ and $\boldsymbol{y}_i$ to output set $\boldsymbol{Y}\subset\boldsymbol{R}$. n is the number of pairs of input and output. The training data are independently and identically generated from a joint probability distribution function $P(\boldsymbol{x}, y)$. The function $h(\boldsymbol{X})$ is to find the dependencies between $\boldsymbol{X}$ and $\boldsymbol{Y}$ in $P(\boldsymbol{x}, y)$ thorough a given regression model (Cord et al. 2009). Eq. (1) can be used for the DME multipath suppression problem as follows. First, the samples of a received DME pulse envelope consist of the input set $\boldsymbol{X}$. The input set includes both of the reference Gaussian and distorted pulses due to noise and multipath. The output set $\boldsymbol{Y}$ consists of the induced TOA (or range) errors corresponding to each pulse in the input set $\boldsymbol{X}$. The modeling of a DME multipath and the preparation of training data are discussed in the following subsection. A received DME signal, $\boldsymbol{x}$, in an interrogator or transponder can be modeled as follows

$$\boldsymbol{x}(t) = \boldsymbol{g}(t) + \boldsymbol{m}(t) + \boldsymbol{\varepsilon}(t) \tag{2}$$

where t is the sample time of a detected DME pulse. $\boldsymbol{g}$ is a transmitted DME pulse. $\boldsymbol{m}$ is a total multipath and $\boldsymbol{\varepsilon}$ is additive white noise. $\boldsymbol{m}$ can be further described as

$$m(t) = \sum_{i=1}^{N} \alpha_i \cos(\phi_i) g(t - \delta_i) \tag{3}$$

where α is the peak amplitude ratio of the multipath to the direct. ϕ is a relative phase difference between the multipath to the direct. δ is the time delay of the multipath. If N is bigger than 1, the resultant multipath will be the sum of N different multipath. i is a index of a multipath. It can be to assumed that α, ϕ, and δ have some finite values. In most cases, α is in the range of (0,1]. Note that ( ) indicates an open interval that excludes the endpoints and [ ] indicates a closed interval that includes the endpoints. The range of ϕ is [0, π] and the range of δ is (0, 6 μs] because the multipath arriving 6 μs behind the direct pulse hardly impacts the timing errors. Based on the range of the parameter values and an arbitrary number of N, it is possible to generate a large number of $\boldsymbol{x}$ that consists of the feature set $\boldsymbol{X}$.

When a modeled DME pulse, $\boldsymbol{x}$, is generated, its peak amplitude may vary. If a multipath is constructive, the peak amplitude of a distorted pulse is bigger than that of the reference Gaussian pulse. Likewise, some distorted pulse may have a lower peak amplitude if a multipath is destructive. To have effective training data set, each $\boldsymbol{x}$ is normalized to one because the pulse should be distinguished by its shape. In addition, $\boldsymbol{x}$ is re-sampled with respect to the determined half amplitude point of $\boldsymbol{x}$ by a sampling time of ΔT_S. The normalized and re-sampled $\boldsymbol{x}$ is denoted as $\boldsymbol{x}_{rs}$. The re-sampling process provides a consistent time slot for the sample points of $\boldsymbol{x}_{rs}$, which helps to better characterize the shape difference among the distorted pulses.

The output set $\boldsymbol{Y}$ consists of TOA errors corresponding to each in the feature set $\boldsymbol{X}$. Using the multipath parameters in Table 2, various training data set of $\boldsymbol{X}$ and $\boldsymbol{Y}$ can be generated as follows

$$\boldsymbol{X} = \begin{bmatrix} x_1(1) & x_1(2) & \cdots & x_1(k) \\ x_2(1) & x_2(2) & \cdots & x_2(k) \\ \vdots & \vdots & \vdots & \vdots \\ x_n(1) & x_n(2) & \cdots & x_n(k) \end{bmatrix} \tag{4}$$
$$\boldsymbol{Y} = \begin{bmatrix} y_1 & y_2 & \cdots & y_n \end{bmatrix}^T.$$

where k is the number of sampling points.

It should be also noted that the feature set $\boldsymbol{X}$ must include some noise that may present in operational environment. It is presumed that the parameter ranges in Table 2 are adequate to represent multipath and noise in most operational conditions. In Table 2, N is set to 2 because the amplitudes of the first and the second multipath are dominant compared to the rest of the following multipath in general. Fig. 2 shows an example of feature training data of $\boldsymbol{X}$ and $\boldsymbol{Y}$ from using the reference Gaussian pulse and

Table 2. Parameter ranges for training data.

Parameter	Ranges
N	2
α_1	0 to 1 in steps of 0.1
ϕ_1	Random, uniform distribution [0, 0.2]
ϕ_2	0 to π
δ_1	Random, uniform distribution [0, π]
δ_2	0 to 6 μs
ε	Random, uniform distribution [δ_1+0.08 μs, δ_1+2 μs]
n	SNR of 25 dB
Sampling	130
frequency	25 MHz

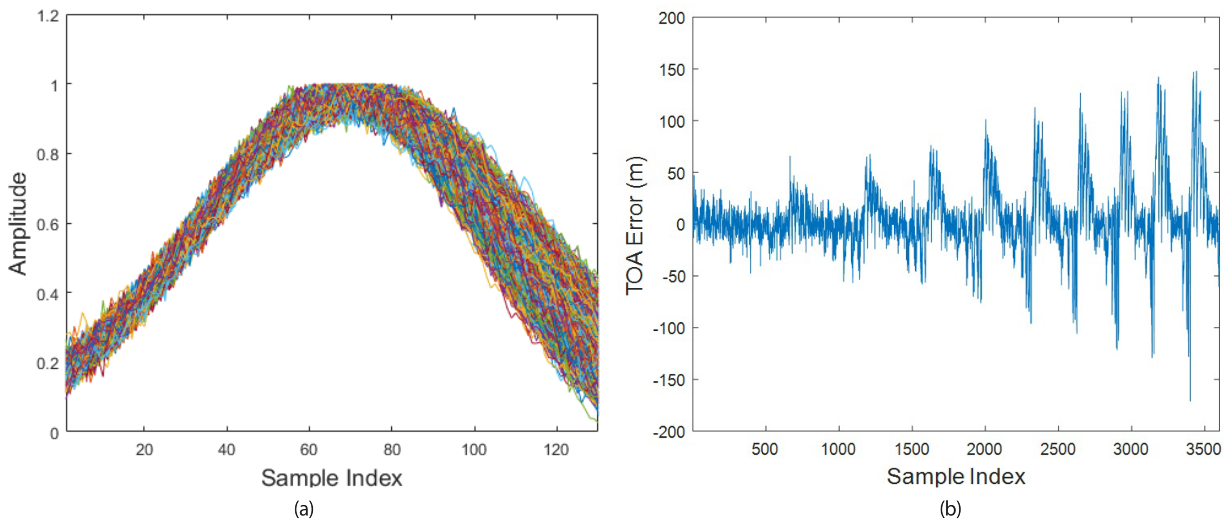

Fig. 2. (a) Training data set of *X* from using the parameter ranges in Table 2. Each training data represents the sum of direct and multipath pulses. (b) Time of Arrival (TOA) errors corresponds to the training data set of *X*.

the multipath parameters in Table 2. Each pulse shown in Fig. 2a represents the sum of the direct and multipath. The increasing trend of the TOA errors in Fig. 2b is because the larger peak amplitude ratio is used as the sample index increases. Note that Fig. 2a and b show the typical value of $\boldsymbol{X}$ and $\boldsymbol{Y}$.

Two linear regression approaches are introduced to find a TOA error predictor using the above training data set in the next section.

2.3 Two Linear Regressions: Least Squares and Regularized Least Squares

To develop a TOA error predictor that helps to suppress multipath impacts, this paper explores the performance of the two linear regression approaches: least squares and regularized least squares. The predictor $\boldsymbol{v}$ for each approach is derived in this section.

Assuming that there is a linear estimator, v, that maps $\boldsymbol{X}$ to $\boldsymbol{Y}$, v can be obtained from using the Least Squares (LS) regression technique as follows

$$\text{minimize}\left\|\boldsymbol{Xv}-\boldsymbol{Y}\right\|_2^2 \tag{5}$$

where $\|\cdot\|_2$ is Euclidean norm. The solution of Eq. (5) is given by the pseudo-inverse of the matrix $\boldsymbol{X}$

$$\boldsymbol{v}_{ls} = \boldsymbol{X}^{\dagger}\boldsymbol{Y} = \left(\boldsymbol{X}^T\boldsymbol{X}\right)^{-1}\boldsymbol{X}^T\boldsymbol{Y} \tag{6}$$

which is a normal equation. Eq. (6) assumes that the number of training data is bigger than the number of the pulse samples.

Now, $\boldsymbol{v}_{ls}$ can be used to estimate a multipath induced TOA error, $\hat{y}$, as follows

$$\hat{y}_{ls} = \boldsymbol{x}_{new}\boldsymbol{v}_{ls} \tag{7}$$

where $\boldsymbol{x}_{new}$ is the sampled points of an arrived DME pulse. When the transmitted DME pulse of $\boldsymbol{x}_{new}$ is identical to the reference DME pulse used in the training data, $\boldsymbol{v}_{ls}$ would be the best estimator providing the minimum residual sum of squares of TOA errors. However, if the transmitted pulse deviates from the reference DME pulse, the estimator wouldn't result in the expected optimal performance.

In order to derive an estimator that also performs well with some uncertainty in the transmitted pulse shapes, Regularized Least Squares (RLS) is preferred to LS. In the RLS formulation, the possible variation in the transmitted pulse can be modeled as uncertainty to the matrix $\boldsymbol{X}$ such that

$$\boldsymbol{A} = \boldsymbol{X} + \boldsymbol{U} \tag{8}$$

where $\boldsymbol{U}$ is a random matrix with a zero mean (Boyd & Vandenberghe 2004). In other words, the matrix $\boldsymbol{A}$ has an average value of $\boldsymbol{X}$ with a certain variance. Then, the problem of the TOA error estimator is formulated as

$$\text{minimize } \mathrm{E}\left\|\boldsymbol{Av}-\boldsymbol{Y}\right\|_2^2 \tag{9}$$

where E stands for expectation. The solution of Eq. (9), $\boldsymbol{v}_{rls}$, is given by

$$\boldsymbol{v}_{rls} = \left(\boldsymbol{X}^T\boldsymbol{X}+\boldsymbol{P}\right)^{-1}\boldsymbol{X}^T\boldsymbol{Y} \tag{10}$$

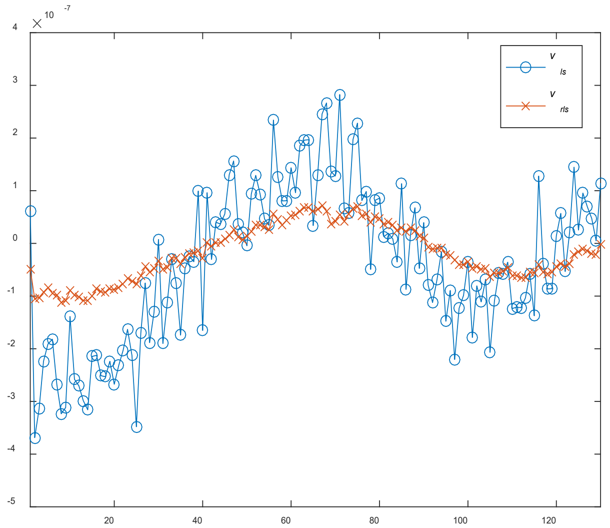

Fig. 3. Comparison of the vector elements of v_{ls} and v_{rls}.

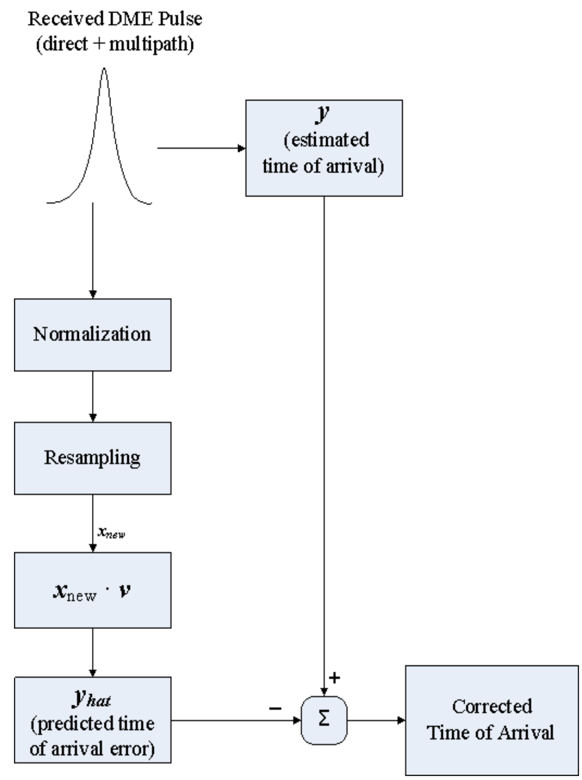

Fig. 4. Multipath rejection process (Kim 2013b).

where $\boldsymbol{P} = \mathrm{E}\boldsymbol{U}^T\boldsymbol{U}$.

The RLS enforces most vector elements of $\boldsymbol{v}_{rls}$ to be smaller than those of $\boldsymbol{v}_{ls}$. For this reason, the $\boldsymbol{v}_{rls}$ may not be as effective as $\boldsymbol{v}_{ls}$ when the reference DME pulse is transmitted. However, the TOA error estimates using $\boldsymbol{v}_{rls}$ would not be sensitive to unexpected DME pulse shapes. Fig. 3 shows one example of the elements of $\boldsymbol{v}_{ls}$ and $\boldsymbol{v}_{rls}$ when $\boldsymbol{P} = 10 \cdot \boldsymbol{I}$ where $\boldsymbol{I}$ is the identity matrix. Note that the values of the vector elements are very small because the value of $\hat{y}$ is the estimated time of arrival in seconds.

3. ASSESSMENT OF MULTIPATH REJECTION PERFORMANCE

This section presents the multipath rejection performance of the proposed method for the following two cases: training data with the reference Gaussian pulse only and training data with the reference Gaussian and non-reference Gaussian pulses. The two cases will show the trade-off between the multipath rejection effectiveness and the allowed waveform variation.

3.1 DME Multipath Rejection Process

The supervised learning is performed offline using either simulation or an actual system. Then, the estimator, $\boldsymbol{v}_{ls}$ or $\boldsymbol{v}_{rls}$, would be stored in a local memory of a DME system. The use of either $\boldsymbol{v}_{ls}$ or $\boldsymbol{v}_{rls}$ will depend on how much the pulse waveform variation can be tightened.

When a DME pulse is received, the procedures shown in Fig. 4 will be executed. The procedure doesn't require heavy computation like other multipath rejection techniques based on iterative searches such as Expectation Maximization (Chan et al. 2005). Upon receiving a DME pulse from an airborne interrogator, a DME ground transponder is given less than 50 μs to perform any computation before sending a reply to the interrogator. Therefore, the simple and fast process in Fig. 4 is an important advantage.

3.2 Simulation Approach: Pulse Waveform Variation and Multipath Generation

The multipath rejection performance of the proposed method would vary depending on the deviation of the transmitted pulse shape from the waveform used in the training data. Therefore, the multipath rejection performance is evaluated against possible variation in the transmitted pulse waveform. For this reason, the multipath performance evaluation is tested under two different cases. The first case only uses the Gaussian reference pulse in the training data. In addition to the reference Gaussian pulse, the second case also includes Gaussian pulses having slightly different standard deviations in the training data. The two cases will result in different multipath TOA error estimators.

The TOA prediction performance is assessed against multipath generated using the same parameters values in Table 1 except that the peak amplitude ratio of the first multipath to the direct, α_1, is limited to 0.5. The reason for this is that α_1 is expected be less than 0.5 in most cases (Kelly & Cusick 1986). However, the estimator was derived by using training data having α_1 up to 1.0 such that some rare multipath having equal or even slightly higher power than the direct would be effectively suppressed as well. Additive white noise under SNR of 30 dB is also injected during the tests. Note that the multipath generated for the test is not the same one used in the training data because of the randomness in the second multipath and additive noise.

Case 1: Learning with Training Data Basis on the Reference Gaussian Pulse

In the first case, the training data uses only the reference Gaussian pulse and corresponding multipath. For the performance evaluation of the LS and RLS estimators, a total of eleven Gaussian pulses are used for the transmitted pulses. The eleven Gaussian pulses include the reference Gaussian pulse and the rest of the ten Gaussian pulses have the rise times varying at ± 100 ns from that of the reference Gaussian pulse. Note that the rise time of a pulse is used as a metric for the waveform variation because it is the most influential parameter to the accuracy of TOA or the half amplitude point estimation in general.

Fig. 5 shows Root Mean Square (RMS) of the raw and compensated TOA errors from using the LS and RLS for the 11 Gaussian pulses. In the figure, the uncompensated TOA errors range from 19.94 to 22.87 meters and tend to slowly escalate as the rise time increases. The TOA errors compensated from the LS based predictor have the minimum RMS of 12.21 m when there is no waveform variation from the reference Gaussian pulse. However, the TOA errors of the LS based predictor quickly diverge as the rise time varies. On the other hand, the RLS based predictor with $\boldsymbol{P} = 10 \cdot \boldsymbol{I}$ provides slightly lesser multipath mitigation of 14.24 m at zero variation. The multipath mitigation of the RLS based predictor also degrades as the rise times of the transmitted pulses diverge. However, the rate of the degradation of the compensated TOA errors is slower than the LS-based predictor.

The main cause of the degradation in both cases is a bias in the TOA measurement caused by the different half amplitude point between the transmitted pulse and the pulse used in the training. Table 3 lists the RMS improvement of the compensated TOA errors from the raw range errors in percent. In the table, the 'X' denotes the cases when the RMS of the compensated range errors from using the LS or RLS is larger than the raw range errors. In other words, the rise time variation corresponding to 'X' should not be allowed when applying the particular LS or RLS based predictors.

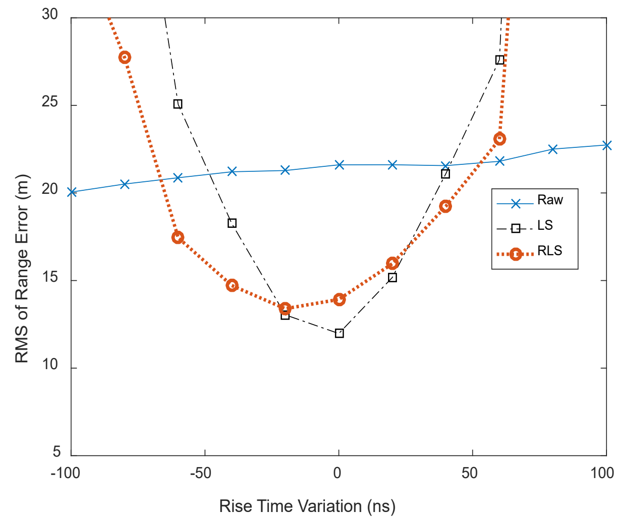

Fig. 5. RMS of multipath range errors of the raw, LS, and RLS with P=10·I.

Table 3. RMS improvement of multipath induced range errors in case 1.

Rise time variation (ns)	LS (%)	RLS (%)
-100	X	X
-80	X	X
-60	X	16
-40	14	31
-20	39	37
0	45	36
20	30	26
40	2	11
60	X	X
80	X	X
100	X	X

Case 2: Learning with Training Data Including non-reference Gaussian Pulse

In the second case, the training data uses the reference and two non-reference Gaussian pulses. One non-reference Gaussian pulse has a slower rise time of 2.75 μs, and the other has a faster rise time of 2.48 μs. The two pairs of the non-reference Gaussian pulses are selected because they can still provide considerable multipath mitigation with large rise time variations. The transmitted pulses for the purpose of the performance test are based on a total of eleven Gaussian pulses. The eleven Gaussian pulses include the reference pulse and the rise times of the remaining ten Gaussian pulses vary at ±250 ns from that of

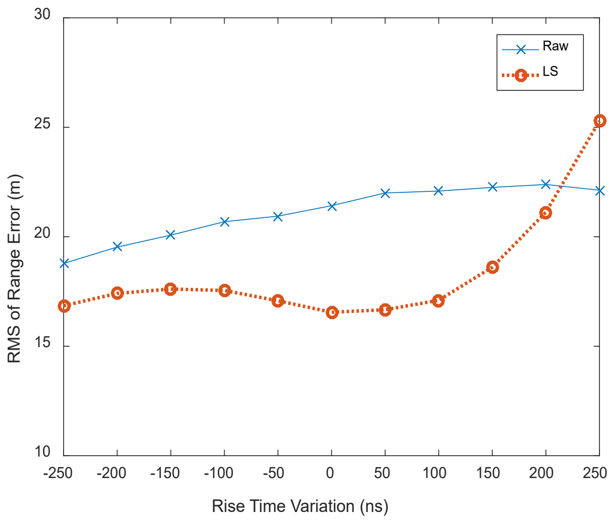

Fig. 6. RMS of multipath range errors of the raw and LS with non-reference Gaussian pulse.

Table 4. RMS Improvement of multipath induced range errors in case 2.

Rise time variation (ns)	LS (%)
-250	10
-200	11
-150	12
-100	15
-50	18
0	22
50	24
100	22
150	16
200	6
250	X

the reference Gaussian pulse.

With the second learning approach, Fig. 6 shows the RMS of the TOA errors of the LS based predictor with respect to the rise time variation. The RLS is not used in the second case because the performance of the RLS and the LS is almost identical in this case. Unlike the case 1, the LS could cover larger rise time variation from -250 to 200 ns but the effectiveness of the multipath mitigation has been reduced. The improvement of the LS based predictor over the raw TOA errors is listed in Table 4.

From the results in the case 1 and case 2, Table 5 summarizes the multipath rejection performance of the proposed method given the range of the allowed rise time variation. The chosen predictor is the one that results in the minimum RMS within the given range of variation. The results clearly show that the proposed method performs better when the rise time variation is minimal. This is a reasonable result because the similarity between the training data and the transmitted signal must be ensured for the validity of the derived estimator from the supervised learning. This results also indicate how much the allowed rise time variation in the current specification needs to be tightened to utilize the proposed method to better suppress DME multipath.

Table 5. Multipath rejection performance given the range of rise time variation.

Rise time variation (ns)	Selected predictor	Mean RMS (m)	RMS improvement over raw range errors (%)
±0	LS in case 1	11.97	45
±20	LS in case 1	13.40	38
±40	RLS in case 1	15.44	28
±100	LS in case 2	17.06	20
±150	LS in case 2	17.35	19
±200	LS in case 2	17.77	16

4. CONCLUSIONS

This paper presented an innovative multipath rejection method of a DME pulse based on the supervised learning. The regression theory of the LS and RLS and the preparation of training data were discussed. The performance of the proposed method was tested in simulation with multipath and noise independently generated from the training data. The results suggest that DME multipath could be effectively suppressed using the proposed method. The performance of the proposed method varies with respect to the pulse shape differences used in the training data and DME operation. When the reference Gaussian pulse was used in the training data and a DME transmitter, the TOA improvement was as high as 45% from the tests. However, as the pulse shape used in transmission deviates from the training data, the improvement of TOA measurement become less effective. With the largest variation of 200 ns, the TOA improvement was 16%.

The results suggest that the DME pulse shape variation should be tightened to mitigate multipath and increase DME range accuracy. Ideally, one particular pulse shape is preferred to be used in both of the transponders and interrogators to maximize the multipath mitigation with the proposed method. Through a software upgrade, ground DME transponders are expected to be able to steadily transmit one particular pulse shape such that unintended pulse waveform variation is lower than noise. Also, the current state-of-the-art avionics should be able to steadily transmit one pulse shape with a software upgrade. However, it may be difficult or impossible to enforce old legacy DME avionics to use one particular pulse shape. For the near term operation, the ground DME transponders would transmit one pulse shape and the DME avionics with updated software would apply the developed estimator to suppress multipath. In this case, multipath mitigation from ground to air only can be provided.

ACKNOWLEDGMENTS

This work was supported by the research grant of Cheongju University in 2015 - 2016.

REFERENCES

Adeli, H. & Ghosh-Dastidar, S. 2010, Automated EEG-based diagnosis of neurological disorders: Inventing the future of neurology (Boca Raton, FL: CRC Press).

Boyd, S. & Vandenberghe, L. 2004, Convex optimization (Cambridge, NY: Cambridge University press).

Carneiro, G., Chan, A. B., Moreno, P. J., &Vasconcelos, N. 2007, Supervised learning of semantic classes for image annotation and retrieval, IEEE transactions on pattern analysis and machine intelligence, 29, 394-410. http://dx.doi.org/10.1109/TPAMI.2007.61

Chan, F., Choi, J., & Jee, G.-I. 2005, Time Estimation of Superimposed Coherent Multipath Signals Using the EM Algorithm for Global Positioning System, Journal of Global Positioning System, 4, 56-64.

Chapelle, O., Schölkopf, B., & Zien, A. 2006, Semi-supervised Learning (Cambridge, MA: MIT Press).

Cord, M., Cunningham, P. & Joshi, D. 2009, Machine Learning Techniques for Multimedia: Case Studies on Organization and Retrieval, Journal of Electronic Imaging, 18, 039901-01-2. http://dx.doi.org/10.1117/1.3207770

Erman, J., Mahanti, A., Arlitt, M., Cohen, I., & Williamson, C. 2007, Semi-supervised network traffic classification, In ACM SIGMETRICS Performance Evaluation Review, 35, 369-70. http://dx.doi.org/10.1145/1254882.1254934

Ghosh-Dastidar, S. & Adeli, H. 2009, A new supervised learning algorithm for multiple spiking neural networks with application in epilepsy and seizure detection, Neural Networks, 22, 1419-1431. http://dx.doi.org/10.1016/j.neunet.2009.04.003

Kayton, M. & Fried, W. R. 1997, Avionics navigation systems, 2nd ed. (New York: John Wiley & Sons).

Kelly, R. J. & Cusick, D. R. 1986, Distance measuring equipment and its evolving role in aviation, Advances in electronics and electron physics, 68, 1-243. http://dx.doi.org/10.1016/S0065-2539(08)60854-9

Kim, E. 2012, Investigation of APNT optimized DME/DME network using current state-of-the-art DMEs: Ground station network, accuracy, and capacity, In Position Location and Navigation Symposium (PLANS), 2012 IEEE/ION, 146-57. IEEE. http://dx.doi.org/10.1109/PLANS.2012.6236876

Kim, E. 2013a, Alternative DME/N pulse shape for APNT, In 2013 IEEE/AIAA 32nd Digital Avionics Systems Conference (DASC), 4D2-1-4D2-10, IEEE. http://dx.doi.org/10.1109/DASC.2013.6712591

Kim, E. 2013b, Enhancing DME/N multipath rejection with tightened pulse waveform variation, In 2013 IEEE/AIAA 32nd Digital Avionics Systems Conference (DASC), 4D1-1-4D1-9, IEEE. http://dx.doi.org/10.1109/DASC.2013.6712590

Lo, S., Chen, Y. H., Segal, B., Peterson, B., Enge, P., et al. 2014, Containing a Difficult Target: Techniques for Mitigating DME Multipath to Alternative Position Navigation and Timing (APNT), In Proceedings of the International Technical Meeting of The Institute of Navigation, San Diego, CA, pp.413-423.

Lo, S., Peterson, B., Akos, D., Narins, M., Loh, R., et al. 2011, Alternative Position Navigation & Timing (APNT) Based on Existing DME and UAT Ground Signals, In Proceedings of the Institute of Navigation GNSS Conference, Portland, OR.

Pelgrum, W., Li, K., Smearcheck, M., & van Graas, F. 2012, eDME architecture development and flight-test evaluation, In 2012 IEEE/AIAA 31st Digital Avionics Systems Conference (DASC), 1-37, IEEE. http://dx.doi.org/10.1109/DASC.2012.6383037

Smaragdis, P. 2007, Convolutive speech bases and their application to supervised speech separation, IEEE Transactions on Audio, Speech, and Language Processing, 15, 1-12. http://dx.doi.org/10.1109/TASL.2006.876726

Euiho Kim is an assistant professor in the department of Aeronautical and Mechanical Engineering in Cheongju University, Chungbuk, Republic of Korea. His current research areas are satellite based navigation, aircraft navigation using ground nav-aids, indoor navigation, and robotics. Previously, Dr. Kim was with the Department of Aerospace Engineering at the University of Kansas as a research associate. He was the technical lead of the Ground-Based Augmentation System (GBAS) of GPS and FAA's Alternative Position, Navigation, and Timing (APNT) programs when he worked in industry. Dr. Kim completed his Ph.D. and master's degree in the department of Aeronautics and Astronautics at Stanford University. He finished his undergraduate degree in the department of Aerospace engineering at Iowa State University.